Developmental Cell, Vol. 5, 723–734, November, 2003, Copyright ©2003 by Cell Press

# Spatial and Temporal Pathway for Assembly and Constriction of the Contractile Ring in Fission Yeast Cytokinesis

**Jian-Qiu Wu,[1] Jeffrey R. Kuhn,[1] David R. Kovar,[1] and Thomas D. Pollard[1,2,*]**

[1]Department of Molecular, Cellular, and Developmental Biology

[2]Department of Cell Biology

Yale University

New Haven, Connecticut 06520

## Summary

**Microscopy of fluorescent fusion proteins and genetic dependencies show that fission yeast assemble and constrict a cytokinetic contractile ring in a precisely timed, sequential order. More than 90 min prior to separation of the spindle pole bodies (SPB), the anillin-like protein (Mid1p) migrates from the nucleus and specifies a broad band of cortex around the equator as the division site. Between 10 min before and 2 min after SPB separation, conventional myosin-II (Myo2p), IQGAP (Rng2p), PCH protein (Cdc15p), and formin (Cdc12p) join the broad band independent of actin filaments. Over the subsequent 10 min prior to anaphase B, this broad band of proteins condenses into a contractile ring including actin, tropomyosin (Cdc8p), and α-actinin (Ain1p). During anaphase B, unconventional myosin-II (Myp2p) joins the ring followed by the septin (Spn1p). Ring contraction and disassembly begin 37 min after SPB separation. This spatial and temporal hierarchy provides the framework for analysis of molecular mechanisms.**

## Introduction

The fission yeast *Schizosaccharomyces pombe* has emerged as a leading model for the analysis of cytokinesis. Not only is it genetically tractable and favorable for microscopic analysis, but it also has the smallest fully sequenced eukaryotic genome and carries out cytokinesis much like animal and protozoan cells. Signals emanating from the nucleus define the position where the cell assembles an equatorial contractile ring of actin filaments, myosin-II, and many associated proteins (Feierbach and Chang, 2001; Guertin et al., 2002; Le Goff et al., 1999; Rajagopalan et al., 2003). At the end of mitosis this ring constricts the plasma membrane at the same time that the cell synthesizes cell wall material to form a septum across the division site. Beginning with Nurse's pioneering work on the cell cycle (Nurse et al., 1976), geneticists have identified more than 50 genes contributing to cytokinesis in *S. pombe* (Feierbach and Chang, 2001; Guertin et al., 2002; Le Goff et al., 1999; Rajagopalan et al., 2003), but biochemical and mechanistic studies have lagged behind the genetics.

The fission yeast contractile ring consists of two type II myosins (heavy chains Myo2p and Myp2p with light chains Cdc4p and Rlc1p; Rajagopalan et al., 2003 and references cited therein), actin filaments (Marks and Hyams, 1985), actin filament crosslinking proteins α-actinin Ain1p and fimbrin Fim1p (Wu et al., 2001), UCS-domain protein Rng3p (Wong et al., 2000), IQGAP Rng2p (Eng et al., 1998), and PCH proteins Cdc15p and Imp2p (Demeter and Sazer, 1998; Fankhauser et al., 1995). Two kinases, Pom1p and Polo kinase Plo1p, and an anillin-like protein Mid1p are involved in correct positioning of the contractile ring (Bähler and Pringle, 1998; Bähler et al., 1998a; Ohkura et al., 1995; Paoletti and Chang, 2000; Sohrmann et al., 1996). Formin Cdc12p, profilin Cdc3p, and tropomyosin Cdc8p are required for assembly of contractile ring actin filaments (Balasubramanian et al., 1992, 1994; Chang et al., 1996, 1997), and formin and profilin cooperate to initiate actin filaments in vitro (Kovar et al., 2003). A signaling cascade including a GTPase and three kinases called the septation initiation network (SIN) regulates septum formation and completion of cytokinesis (Guertin et al., 2002).

Although one can piece together from diverse papers an approximate temporal sequence of events during the assembly and constriction of the fission yeast contractile ring, the actual sequence of events has not been established. Furthermore, gaps exist in the genetic tests for dependencies among the proteins that participate in cytokinesis. In addition, some published reports disagree about important features. Because knowledge of the order of events and the genetic dependencies along the pathway of contractile ring assembly and constriction are prerequisites for deciphering the underlying molecular mechanisms, we used a large set of fluorescent fusion proteins to refine the spatial, temporal, and genetic landscape for cytokinesis in fission yeast.

## Results

We used time-lapse microscopy to investigate the assembly and constriction of the cytokinetic contractile ring in fission yeast strains expressing 14 proteins tagged on their $NH_2$ and/or COOH termini with fluorescent proteins GFP, YFP, or CFP. Most tagged genes were integrated at their chromosomal loci under the control of native promoters. We ruled out partial loss of function by examining colony formation and cellular morphology and/or by crossing tagged strains with mutant strains known to have synthetic interactions with mutations in the tagged gene (Experimental Procedures). CFP-tubulin (Atb2p; Glynn et al., 2001), tropomyosin GFP-Cdc8p (M. Balasubramanian, personal communication) and YFP-Cdc8p, and formin Cdc12p-CFP (F. Chang, personal communication) were expressed from plasmids under the control of *nmt1* promoters (*3nmt1* for tubulin and medium strength *41nmt1* for others). We observed many cells of each strain and analyzed 6–20 cells in detail (Figures 1–4; Supplemental Table S1 and Movies are available at http://www.developmentalcell.com/cgi/content/full/5/5/723/DC1).

*Correspondence: thomas.pollard@yale.edu

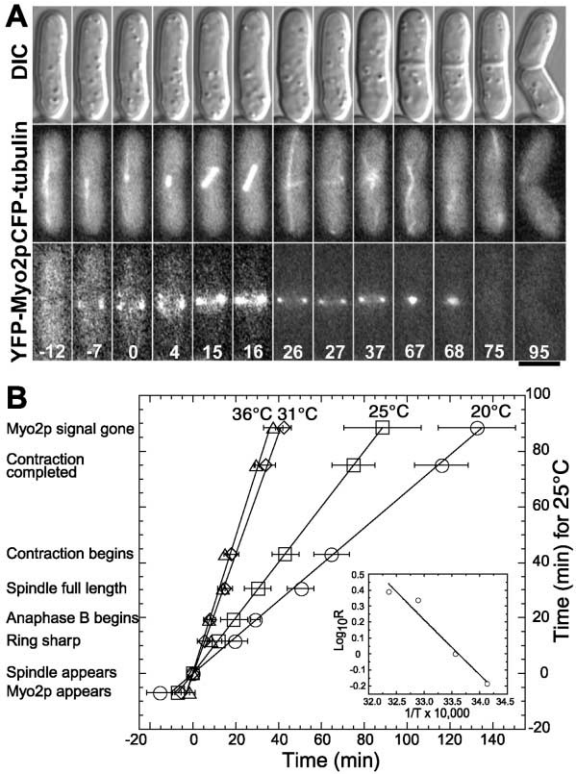


Figure 1. Temperature Dependence of Mitotic and Cytokinetic Events Observed by Time-Lapse Microscopy

(A) DIC and fluorescence micrographs of fission yeast expressing YFP-Myo2p and CFP-tubulin (JW923). This cell was grown in minimal medium EMM2 plus 0.2 μM thiamine and photographed every min at 25°C in this medium with 2% agar. Elapsed time is shown in minutes. Time zero is the first frame with a spindle. The scale bar (for this and all other figures) represents 5 μm.

(B) Temperature dependence of the time course of mitotic and cytokinetic events. The y axis is the time of events (listed on the left) at 25°C. The x axis is the observed time of the events at 20°C, 25°C, 31°C, and 36°C, with "spindle appears" defined as time zero. Error bars are ± 1 standard deviation. The inset is an Arrhenius plot of $\log_{10}R$ (rate of mitosis and cytokinesis) versus 1/T (degree Kelvin) × $10^4$.

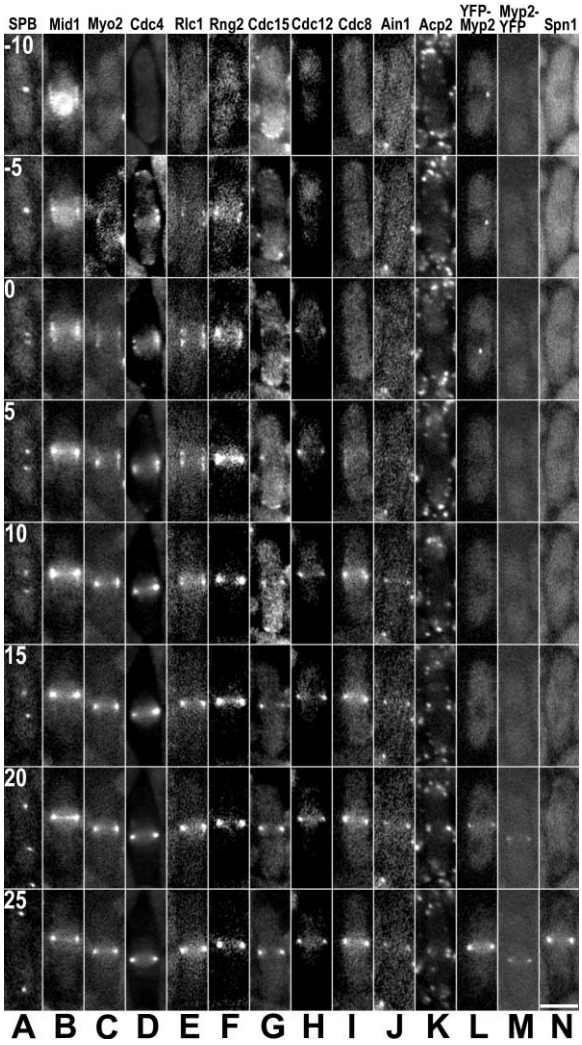


Figure 2. Time Course of the Localization of Cytokinesis Proteins Observed by Time-Lapse Fluorescence Microscopy

(A–N) Cells expressing YFP- and CFP-fusion proteins were grown on EMM2 plus 25% gelatin at 25°C and photographed every min except (B) (every 2 min) and (C) and (F) (every 1.5 min). Representative cells are shown at ~5 min intervals. The first time when two SPBs marked with Sad1p were resolved as separate dots is defined as time zero. Representative series can be viewed in Supplemental Movies 1 and 2.

(A) SPBs from strain *rlc1-YFP sad1-CFP* (JW991). SPBs in all other strains behaved similarly and are not shown.

(B) Anillin-like protein Mid1p in strain *mid1-YFP sad1-CFP* (JW820).

(C) Conventional type II myosin Myo2p in strain *YFP-myo2 sad1-CFP* (JW834).

(D) Myosin-II essential light chain Cdc4p in strain *YFP-cdc4 sad1-CFP* (JW946).

(E) Myosin-II regulatory light chain Rlc1p in strain *rlc1-YFP sad1-CFP* (JW991).

(F) IQGAP Rng2p in strain *YFP-rng2 sad1-CFP* (JW931).

(G) PCH protein Cdc15p in strain *cdc15-YFP sad1-CFP* (JW979).

(H) Formin Cdc12p in strain *cdc12-CFP sad1-YFP* (JW788).

(I) Tropomyosin Cdc8p in strain *YFP-cdc8 sad1-CFP* (JW952).

(J) α-actinin Ain1p in strain *ain1-YFP sad1-CFP* (JW984).

(K) Capping protein Acp2p in strain *acp2-YFP sad1-CFP* (JW932).

(L) Unconventional myosin-II Myp2p in strain *YFP-myp2 sad1-CFP* (JW935).

(M) Unconventional myosin-II Myp2p in strain *myp2-YFP sad1-CFP* (JW784).

(N) Septin Spn1p in strain *spn1-CFP sad1-YFP* (JW981).

## Fission Yeast Cytokinesis Clock

To provide a frame of reference for quantitative analysis of cytokinesis, we determined the timing of key events at 25°C (Figures 1 and 2; see Supplemental Table S1 for sample sizes and variability). DIC micrographs showed cell size, septation, and separation. Fluorescence micrographs of cells expressing two fluorescent fusion proteins allowed simultaneous visualization of 12 different contractile ring proteins (Figure 2; Supplemental Movies 1 and 2) and either the intranuclear mitotic apparatus labeled with CFP-tubulin (Figure 1A) or spindle pole bodies (SPB) labeled with CFP- or YFP-Sad1p (Figure 2A; Supplemental Table S1). The interphase SPB migrates in the cytoplasm close to the nucleus until mitosis, when it incorporates into the nuclear envelope (Ding et al., 1997).

Key events are separation of SPBs at the onset of mitosis (defined as time zero; Nabeshima et al., 1998), beginning of anaphase B (mean time 9.2 min; first frame

with spindle length > 2.5 μm; Mallavarapu et al., 1999; Nabeshima et al., 1998), completion of anaphase B separation of SPBs (29.4 min), beginning of contraction and initial appearance of a septum (36.5 min), and cell separation (101.9 min) (Figure 4B). No individual strain (Supplemental Table S1) deviated from the average of all strains. YFP conventional myosin-II (Myo2p) allowed tracking of the parallel cytokinetic events (Figures 1A and 2C): formation of a broad band of Myo2p at the division site (−7 min); coalescence of Myo2p into a sharp equatorial ring between min 4 and 13; initiation of ring contraction (37 min); completion of constriction (67 min); and disassembly of the Myo2p ring by dispersion in the cytoplasm or into dots or filaments near the septum over about 14 min. This timing is very similar to the untagged wild-type strain (JW729) tested under same conditions, which took 64.0 min (n = 13 cells) from septum appearance to cell separation.

### Dependence of the Cytokinesis Clock on Temperature

We used the 25°C time scale as the standard to compare the timing of the mitotic and cytokinetic events at 20°C, 31°C, and 36°C (Figure 1B). In this plot, the y axis is the timing of events at 25°C and the x axis is the observed time of the events. All of the scored events occurred in exactly the same linear temporal sequence at all temperatures tested, with rates dependent on the temperature. An Arrhenius plot of the rates is linear (Figure 1B, inset), with an activation energy of 16 kcal/mol.

### Three Stages in the Assembly of the Cytokinetic Contractile Ring

Assembly of the contractile ring takes place in three stages. The order of these events can be viewed in time-lapse movies (Figures 2 and 3; summarized in Figure 4B; Supplemental Movies 1–3), kymographs (Figure 4A), and single micrographs of fields of asynchronous cells expressing pairs of fluorescent fusion proteins (Figure 5). Each method has certain advantages and together they provide a consistent account of the events.

In the first stage, anillin-like protein (Mid1p) exits from the nucleus and marks a broad equatorial domain of the cellular cortex, where it is joined sequentially during the G2/M transition by myosin-II, IQGAP (Rng2p), PCH protein (Cdc15p), and formin (Cdc12p) (Figure 2). Mid1p accumulates in the nucleus during most of interphase. At least 90 min before mitosis, Mid1p begins to move to a broad cortical band adjacent to the nucleus until the transfer is complete 2.0 min after SPB separation (Figure 2B). During most of interphase, the subunits of conventional myosin-II (heavy chain Myo2p, light chains Cdc4p and Rlc1p) and IQGAP Rng2p are spread throughout the cytoplasm (Figures 2C–2F and 3A, top right cell). (We did not observe YFP-Rng2p to concentrate on SPBs like GFP-Rng2p expressed from a plasmid [Eng et al., 1998]; also see Figure 6B). Six to nine minutes before SPB separation, the myosin-II subunits and Rng2p begin to accumulate in a broad equatorial band (Figures 2C–2F). This is earlier than all published reports (Bezanilla et al., 2000; Eng et al., 1998; Motegi et al., 2000). Myo2p is organized into 50–100 discrete dots

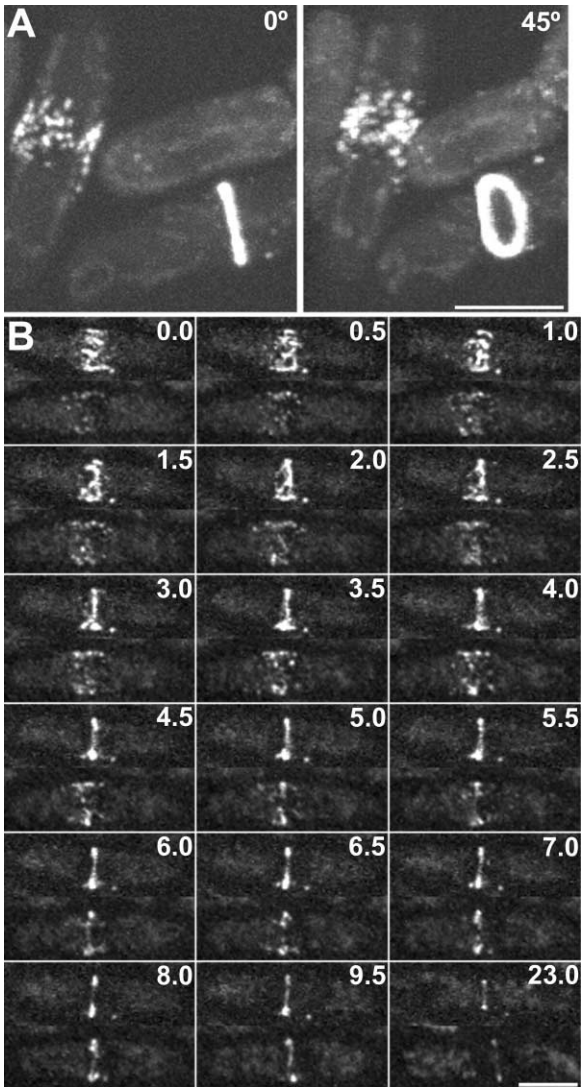


Figure 3. Time Course of the Assembly of Conventional Myosin-II Myo2p into a Contractile Ring Observed by Spinning Disk Confocal Fluorescence Microscopy of Strain JW766 Expressing GFP-Myo2p

(A) Images of Myo2p in three cells from a stack of 51 confocal z-sections of 0.1 μm viewed at 0° and 45° to the y axis. Myo2p forms a broad equatorial band in the cell on the left and a compact contractile ring in the cell on the right.

(B) A time-lapse series of two cells at intervals of 0.5 min. A stack of 31 z-sections of 0.2 μm was taken at each time point and projected as a 2D image. Before the first frame, Myo2p in the upper cell formed a broad band that coalesced into a contractile ring at 4 min. The lower cell was about 2 min behind the upper cell. The entire series can be viewed in Supplemental Movie 3.

(Figure 3A, left cell) that subsequently coalesce into linear structures (Figure 3B; Supplemental Movie 3) that are not evident by conventional microscopy (Figure 2C). By 2 min, two proteins contributing to actin polymerization appear at the cleavage site: PCH protein (Cdc15p) and formin (Cdc12p) (Figures 2G and 2H). The original work (Fankhauser et al., 1995) emphasized concentration of Cdc15p in the contractile ring, while we also find Cdc15p in dots near the ends of interphase cells in agreement with concurrent work (Carnahan and Gould,

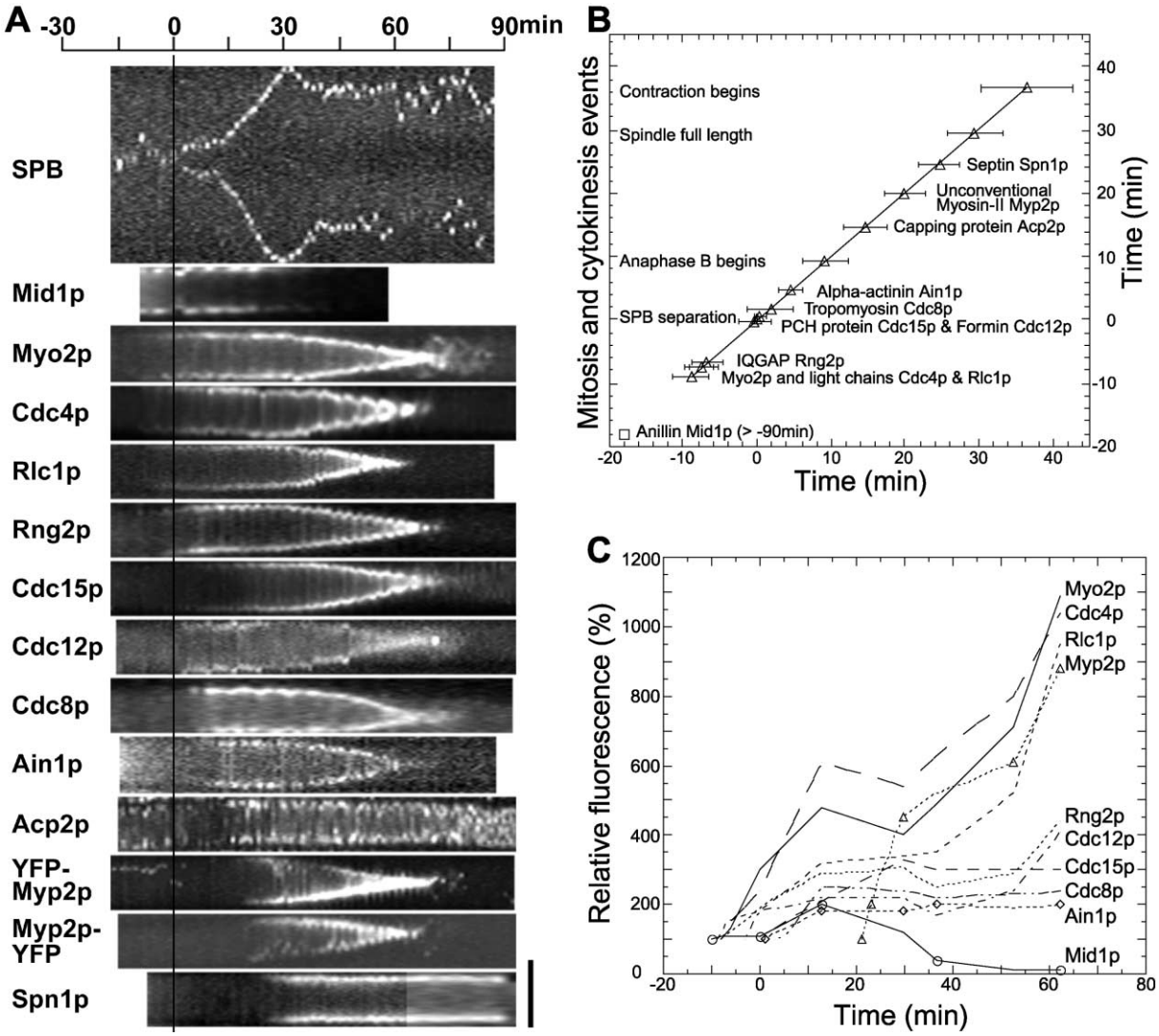


Figure 4. Time Course of the Assembly, Constriction, and Disassembly of the Contractile Ring at 25°C

(A) Kymographs showing SPB movements and assembly, constriction, and disassembly of the contractile ring in cells expressing Sad1p-CFP or Sad1p-YFP to mark SPBs and cytokinesis proteins tagged with YFP or CFP. Kymographs were constructed using Image J. SPB kymographs were constructed with a 13.7 μm slit parallel to the long axis of the cell to document the separation of the SPBs and cell cycle stage (top). Kymographs of contractile ring proteins were constructed with a 4.1 μm slit cross the midplane of the cell. Kymographs were aligned at the time of SPB separation (vertical line).

(B) Time course of the first appearance of cytokinesis proteins at the cleavage site. The line is the time course of mitotic and cytokinetic events (listed to the left) at 25°C similar to Figure 1, with SPB separation defined as time zero. The mean time of the appearance of each protein in time-lapse movies (Figure 2; Supplemental Table S1) is plotted along this time line. Error bars are ± 1 standard deviation. Anillin (Mid1p) appeared at the equatorial cortex > 90 min before SPB separation.

(C) Time course of changes in the relative fluorescence intensity in the contractile ring of ten proteins tagged with YFP or CFP. One representative cell was analyzed for each protein. The peak fluorescence intensity as shown in Supplemental Figure S1 is plotted against time (SPB separation is time zero). The intensity 2 min before each signal appeared at the equator is set at 100%.

2003). These dots begin moving to the division site as SPBs separate, and finish during anaphase.

During the second stage two major events occur between 2 and 10 min. First, actin polymerizes in the broad band and binds tropomyosin Cdc8p (Figure 2I). We know actin polymerizes at this time from previous work on fixed cells (Arai and Mabuchi, 2002) and from the accumulation of tropomyosin, which only binds polymerized actin. We did not document actin polymerization directly in live cells, because no tagged actin construct that we tested incorporated into contractile ring filaments (in spite of concentrating in actin patches). Second, the broad band consisting of anillin Mid1p, myosin-II (Myo2p, Cdc4p, and Rlc1p), IQGAP Rng2p, PCH protein Cdc15p, formin Cdc12p, actin, tropomyosin Cdc8p, and α-actinin Ain1p (Figure 2J) condenses into a sharp, continuous contractile ring (Figures 2 and 3A, bottom right cell). This compaction takes about 10 min and is completed by the beginning of anaphase B.

During the third stage, lasting about 25 min during

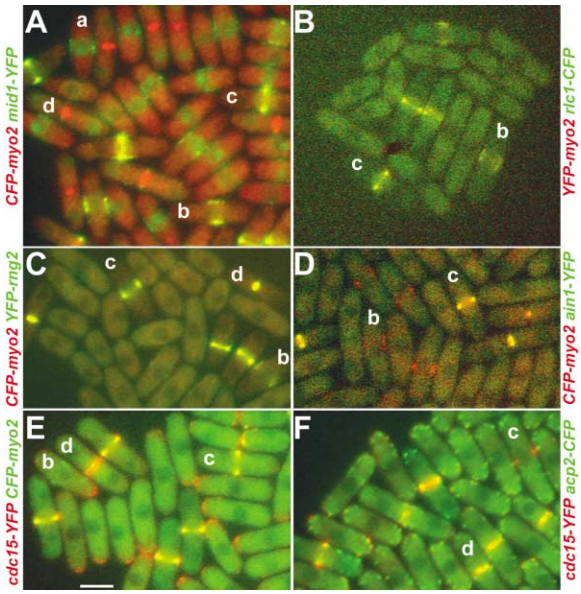


Figure 5. Fluorescence Micrographs of Asynchronous Populations of Fission Yeast Expressing Pairs of Fluorescent Fusion Proteins

(A–F) Cells were photographed with YFP and CFP filters and the images were merged. Colocalized signals are yellow. White letters on the figures highlight protein(s) in (a) nucleus and broad equatorial band, (b) broad equatorial band, (c) contractile ring, and (d) constricted contractile ring.

(A) Mid1p-YFP CFP-Myo2p (JW851).
(B) Rlc1p-CFP YFP-Myo2p (JW968).
(C) YFP-Rng2p CFP-Myo2p (JW928).
(D) Ain1p-YFP CFP-Myo2p (JW986).
(E) CFP-Myo2p Cdc15p-YFP (JW980).
(F) Acp2p-CFP Cdc15p-YFP (JW995).

anaphase B, the compact contractile ring maintains a constant diameter but matures by addition of unconventional myosin-II Myp2p (Figures 2L and 2M). Myp2p joins the contractile ring 29 min after Myo2p in stain JW835 expressing CFP-Myo2p and Myp2p-YFP from native promoters, in agreement with experiments on two strains expressing GFP myosins (Bezanilla et al., 2000) rather than simultaneously (Motegi et al., 2000). A dot of YFP-Myp2p (Figure 2L) and actin patches containing capping protein Acp2p-YFP (Figure 2K) produce intermittent signals in kymographs when they pass near the equator before time zero (Figure 4A). Actin patches cluster near the ring in anaphase B and a small fraction of the capping protein joins the ring (Figure 2K). The septin Spn1p concentrates near the ring late in anaphase B (Figure 2N).

Micrographs of fields of unsynchronized cells expressing fluorescent Myo2p and a second fluorescent fusion protein confirmed the order of events and provide additional details (Figure 5). The distributions of several proteins overlap throughout the cell cycle: the fluorescence from the heavy chain of conventional myosin-II Myo2p (Figures 5B and 5C), myosin light chains Rlc1p (Figure 5B) and Cdc4p, and IQGAP Rng2p (Figure 5C) shift from the interphase cytoplasm to the broad equatorial band to the contractile ring and remain together as the ring constricts.

Dual expression of other proteins illustrates their independent behavior. Anillin Mid1p moves from the nucleus to the broad equatorial band well before Myo2p (Figure 5A, cell a). Later their signals overlap when Myo2p joins Mid1p in the broad band (Figure 5A, cell b). During early mitosis, dots of both proteins coalesce to form a well-organized ring (Figure 5A, cell c). Mid1p does not contract with the Myo2p ring, but fades in overall intensity and relocalizes to both daughter nuclei (Figure 5A, cell d). $\alpha$-actinin Ain1p joins Myo2p as it forms the compact ring (Figure 5D, cell c). PCH protein Cdc15p joins the contractile ring later than Myo2p (Figure 5E, cell b) but earlier than Acp2p (Figure 5F, cell c). During interphase, Cdc15p concentrates in dots that overlap incompletely with actin patches marked with capping protein Acp2p (Figure 5F).

### Steps in Contractile Ring Assembly Dependent on Polymerized Actin

We used Latrunculin A (Lat-A) to depolymerize actin filaments (Ayscough et al., 1997) in cells expressing fluorescent fusion proteins (Figure 6E). We either added Lat-A to asynchronous cells or used the temperature-sensitive strain *cdc25-22* to observe the effects of Lat-A on synchronized cells released from arrest at G2/M. Lat-A depolymerizes actin filaments in patches, cables, and contractile rings in less than 5 min but this does not prevent anillin (Mid1p; Paoletti and Chang, 2000), conventional myosin-II (Myo2p, Cdc4p, and Rlc1p), IQGAP (Rng2p), formin (Cdc12p), or PCH protein (Cdc15p) from accumulating around the equator (Figure 6; Supplemental Table S2). However, the broad equatorial bands of these proteins fail to form tight rings and the cells do not cleave in Lat-A. Depolymerization of actin filaments does not disperse Cdc15p dots at the cell tips. On the other hand, depolymerization of actin filaments prevents localization of tropomyosin (Cdc8p), $\alpha$-actinin (Wu et al., 2001), capping protein (D.R.K. et al., unpublished), and unconventional myosin-II (Myp2p) to the cleavage site and stops the progression of cytokinesis in cells with fully formed contractile rings. DMSO, the carrier for Lat-A, has no effect on the localization of test proteins (Figures 6B and 6D–6G, and data not shown; Supplemental Table S2).

We confirm that actin filaments are not required for Myo2p dots to accumulate at the equator (Motegi et al., 2000) or to maintain Myo2p at the ring site once formed (Naqvi et al., 1999). However, the Myo2p ring is fragmented and discontinuous without actin filaments. When the *cdc25-22 rlc1-GFP* strain (JW877-1) is arrested and treated with Lat-A and then released into Lat-A, Rlc1p accumulates in a broad band of dots but fails to condense into a compact contractile ring or to constrict a cleavage furrow. Similarly, in *rlc1-YFP* cells, Lat-A arrests partially contracted rings for over 41 min (Figure 6C, left cell) and prevents broad bands of Rlc1p from coalescing into compact rings for at least 2 hr (Figure 6C, right cell). Similar images were obtained from three other cells and from cells tagged with YFP-Cdc4p Sad1p-CFP (JW946).

Actin filaments are not required for IQGAP Rng2p to accumulate at the division site, but are required to form and maintain an intact ring of Rng2p. After release into Lat-A, 82% of *YFP-rng2 cdc25-22* cells ($n = 312$) form a broad band of Rng2p at the division site (Figure 6A)

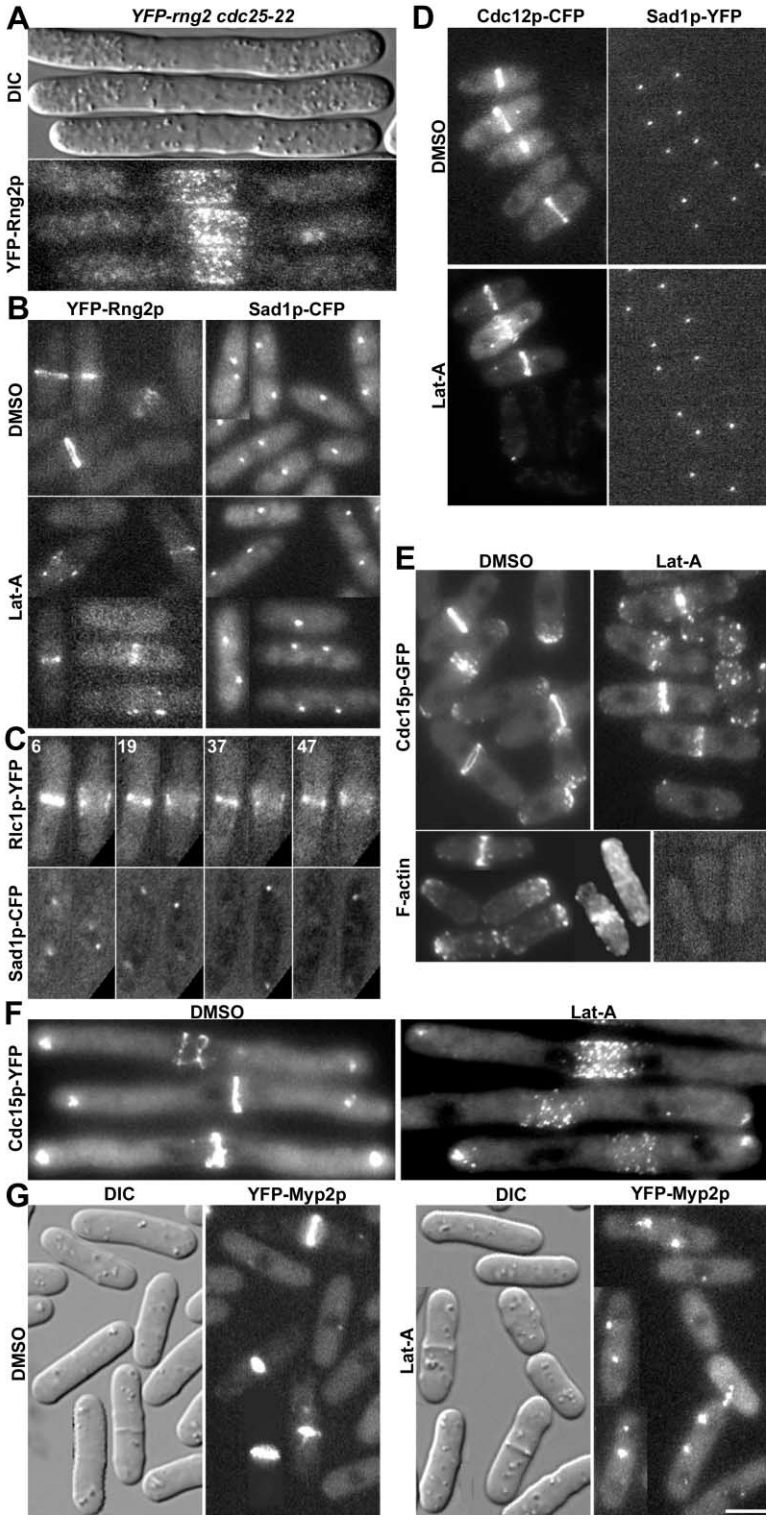


Figure 6. Fluorescence and DIC Micrographs of Cells Treated with 100 μM Latrunculin A (Lat-A) to Determine Whether Localization of Contractile Ring Proteins Depends on Polymerized Actin

DMSO indicates controls treated with the carrier for Lat-A.

(A) Localization of IQGAP Rng2p in synchronized cells. Strain *YFP-rng2 cdc25-22* (JW971-1) was arrested at 36°C for 4 hr, incubated in Lat-A at 36°C for 30 min, and released to 23°C for 2 hr in Lat-A. Sixteen fluorescence z-sections spaced at 0.5 μm were projected into a 2D image using a maximum intensity projection.

(B) Localization of IQGAP Rng2p and SPB marker Sad1p in asynchronous cells. Strain *YFP-rng2 sad1-CFP* (JW931) was treated with Lat-A or DMSO for 90 min at 25°C. Eight z-sections spaced at 0.7 μm were projected into 2D images using a maximum intensity projection.

(C) Localization of myosin regulatory light chain Rlc1p and Sad1p in asynchronous cells. Strain *rlc1-YFP sad1-CFP* (JW991) was treated with Lat-A at time zero at 25°C. Cells were spotted onto a slide without gelatin and sealed with Valap. Fluorescence micrographs were recorded at 1 min intervals. At 6 min, the left cell had a ring and the right cell had a broad band.

(D) Localization of formin Cdc12p and Sad1p in asynchronous cells. Strain *cdc12-CFP sad1-YFP* (JW788) grown under inducing conditions for *41nmt1-cdc12-CFP* for 22 hr was treated with Lat-A or DMSO for 30 min at 25°C. Image processing as in (B).

(E) Localization of PCH protein Cdc15p and actin filaments in asynchronous cells. Strain *cdc15-GFP* (JW976) was treated with Lat-A or DMSO for 30 min at 25°C. Upper panels: micrographs of live cells with an FITC filter. Lower panels: samples fixed and stained with rhodamine-phalloidin to visualize actin filaments. Image processing as in (B).

(F) Localization of PCH protein Cdc15p in synchronized cells. Strain *cdc25-22 cdc15-YFP sad1-CFP* (JW1012) was synchronized and treated with Lat-A as in (A). The micrograph of the DMSO control was taken 30 min after shifting to 23°C to show intermediate stages of ring formation. The micrograph of the cells treated with Lat-A was taken 2 hr after shifting to 23°C.

(G) Localization of unconventional myosin-II Myp2p in asynchronous cells. Strain *YFP-myp2* (JW916) treated with Lat-A or DMSO for 50 min at 25°C. Image processing as in (B). Strain *myp2-GFP* (JW706) treated with Lat-A for 5 min gave similar results.

that persists for at least another 2 hr without forming a compact ring. Similarly, a broad band or ring of Rng2p persists for up to 4 hr in asynchronous *YFP-rng2* cells treated with Lat-A (Figure 6B). However, in Lat-A, the Rng2p rings are not continuous and smooth like in controls. This differs from Eng et al. (1998), who reported that polymerized actin is required for IQGAP Rng2p to localize to the contractile ring.

Lat-A has little effect on the localization of Cdc12p to the division site in 30 min (Figure 6D), but over the next 2 hr the rings fragment into many dots around the equator. A few of these dots move by themselves or with SPBs. Thus, actin filaments are not required to maintain Cdc12p at the division site.

Actin filaments are not required for Cdc15p to accumulate at the division site, but are required to form and

maintain an intact ring of Cdc15p. Although Lat-A destroys all actin patches and rings in less than 5 min, Cdc15p retains its punctate distribution at the ends of interphase cells and around the equator of dividing cells (Figure 6E). No cells have continuous, smooth rings of Cdc15p such as those in control cells (Figure 6E). These dots of Cdc15p persist at the equator for up to 3 hr in Lat-A, although they become more scattered. After release into Lat-A, 94% of *cdc15-YFP cdc25-22* cells (n = 329) form a broad band of Cdc15p at the division site (Figure 6F) that persists for at least another hour without forming a compact ring. In contrast, cells treated with DMSO form a broad band, filaments, a contractile ring, and a septum starting from 25 min after release to 23°C (Figure 6F).

In contrast to the proteins that arrive early at the equator in preparation for cytokinesis, Lat-A prevents targeting of tropomyosin (Cdc8p), α-actinin (Wu et al., 2001), capping protein (D.R.K. et al., unpublished), and unconventional myosin-II (Myp2p) to the contractile ring. Lat-A disperses tropomyosin GFP-Cdc8p expressed from a plasmid (strain JW951) from the contractile ring, actin cables, and patches within 2 min (n = ~5000 cells). Similarly, Lat-A disperses YFP-Myp2p (Figure 6G; n = ~4,000 cells) and Myp2-GFP (n = ~4,000 cells) from the contractile ring. YFP-Myp2p accumulates in two or more dots, Myp2-GFP disperses in the cytoplasm of most cells, but a few have dots of fluorescence (Figure 6G and data not shown). Similarly, Lat-A prevents the localization of Myp2p to equatorial bands or rings during 3 hr after release of *myp2-GFP cdc25-22* cells (strain JW876-1; n = ~2,000 cells) from G2/M arrest.

### Constriction and Disassembly of the Contractile Ring

Kymographs (Figure 4A) and scans of fluorescence intensity (Supplemental Figure S1; Figure 4C) are useful for tracking the constriction and disassembly of the contractile ring. We distinguish three patterns.

First, the local fluorescence intensity of Myo2p heavy chain and the two light chains (Cdc4p and Rlc1p) increases as the broad band coalesces into the contractile ring (Figure 4C). Fluorescence intensity is constant during anaphase B and then nearly triples as the ring constricts to a dot. Thus, the local concentration of myosin-II increases as the volume of the ring decreases during constriction. Thereafter myosin-II fluorescence drops suddenly as the ring fragments into dots or filaments, which disperse as general cytoplasmic fluorescence over 22 min.

Myp2p joins the ring later than Myo2p but also increases in intensity during constriction (Figure 4C). The irregular distribution of Myp2p fluorescence in the ring (Bezanilla et al., 2000) appears as asymmetry in the kymographs (Figure 4A). After ring contraction, Myp2p usually splits into two or more dots, which move away from the division site and move around in each daughter cell. Dots of Myp2-YFP disappear within 14 min after contraction (Figure 4A). On the other hand, dots of YFP-Myp2p persisted an average of 20 min in five of nine cells examined and more than 50 min in four other cells, as reported for overexpressed GFP-Myp2p (Bezanilla et al., 2000).

Second, the fluorescence intensity of Rng2p, Cdc12p, and Cdc15p in the contractile ring increases 2- to 3-fold from early mitosis to spindle breakdown at the end of anaphase B. As the ring constricts, the local fluorescence intensity of Rng2p and Cdc12p increases slightly but that of Cdc15p is constant (Figure 4C). After ring contraction, Cdc15p relocalizes to dots near the newly formed septum (Figures 5E and 5F). Ain1p and Cdc8p are similar to Cdc15p: their fluorescence intensities increase as the ring matures during early mitosis and remain constant as the ring contracts to a dot (Figure 4C). This behavior indicates that Cdc15p, Ain1p, and Cdc8p are lost in proportion to the decline in volume of the ring as it constricts.

Third, anillin Mid1p, capping protein Acp2p, and the septin Spn1p do not constrict with the contractile ring, although their fates differ (Figure 4A). The cortical fluorescence of Mid1p drops dramatically during anaphase B and disappears from the medial cortex 13 min after the contractile ring begins to constrict (Figure 4C). The capping protein signal is too faint to observe constriction of the ring relative to the strong signal from cortical patches near the equator (Figure 4A). The septin remains as rings flanking the septum after ring contraction (Figure 4A).

### Genetic Dependencies of Steps in Contractile Ring Assembly and Constriction

Many genetic dependencies for cytokinesis in *S. pombe* had not been tested, so we used temperature-sensitive or deletion mutants to learn more about this functional hierarchy and confirm the spatial and temporal pathway (Figure 7; Supplemental Table S2).

Normal localization of Myo2p and Rng2p to the broad equatorial band and contractile ring depends on Mid1p. The *mid1* gene is not essential for viability (Paoletti and Chang, 2000; Sohrmann et al., 1996), but deletion of *mid1* profoundly disturbs the behavior of Myo2p (Figure 7A; Supplemental Movies 4 and 5). *mid1*Δ cells begin to accumulate Myo2p dots and/or filaments instead of a broad band 4.5 ± 3.2 min (n = 7 cells) after SPB separation (13 min later than in *mid1*$^+$ cells), but they are not confined to the equator. Some of these cells fail to assemble a Myo2p ring; most make a misplaced, defective ring that slowly contracts and guides septation. Treatment with Lat-A disrupts these rings into fragmented rings or cables. IQGAP Rng2p behaves very similarly to Myo2p in *mid1*Δ cells.

Formation of a contractile ring but not a broad band of Rng2p depends on Cdc12p. YFP-Rng2p is fully functional at 36°C, because the time course of mitosis and cytokinesis in this strain (Figure 7B; n = 10 cells) is very similar to untagged wild-type cells at 36°C. At the restrictive temperature, *YFP-rng2 cdc12-112* cells accumulate Rng2p at the division site, but do not form a compact contractile ring (Figure 7C; n = 11 cells). No septa form in 3 hr, confirming the loss of Cdc12p function at 36°C.

Localization of Rng2p to the equator depends on myosin light chain Cdc4p. At the restrictive temperature of 36°C, *YFP-rng2 cdc4-8* cells do not accumulate Rng2p at the division site, although some cells make aberrant partial septa (Figure 7D). Some cells have one or two weak, motile fluorescent dots, perhaps improperly assembled Rng2p from a previous cell cycle (Figure 7D).

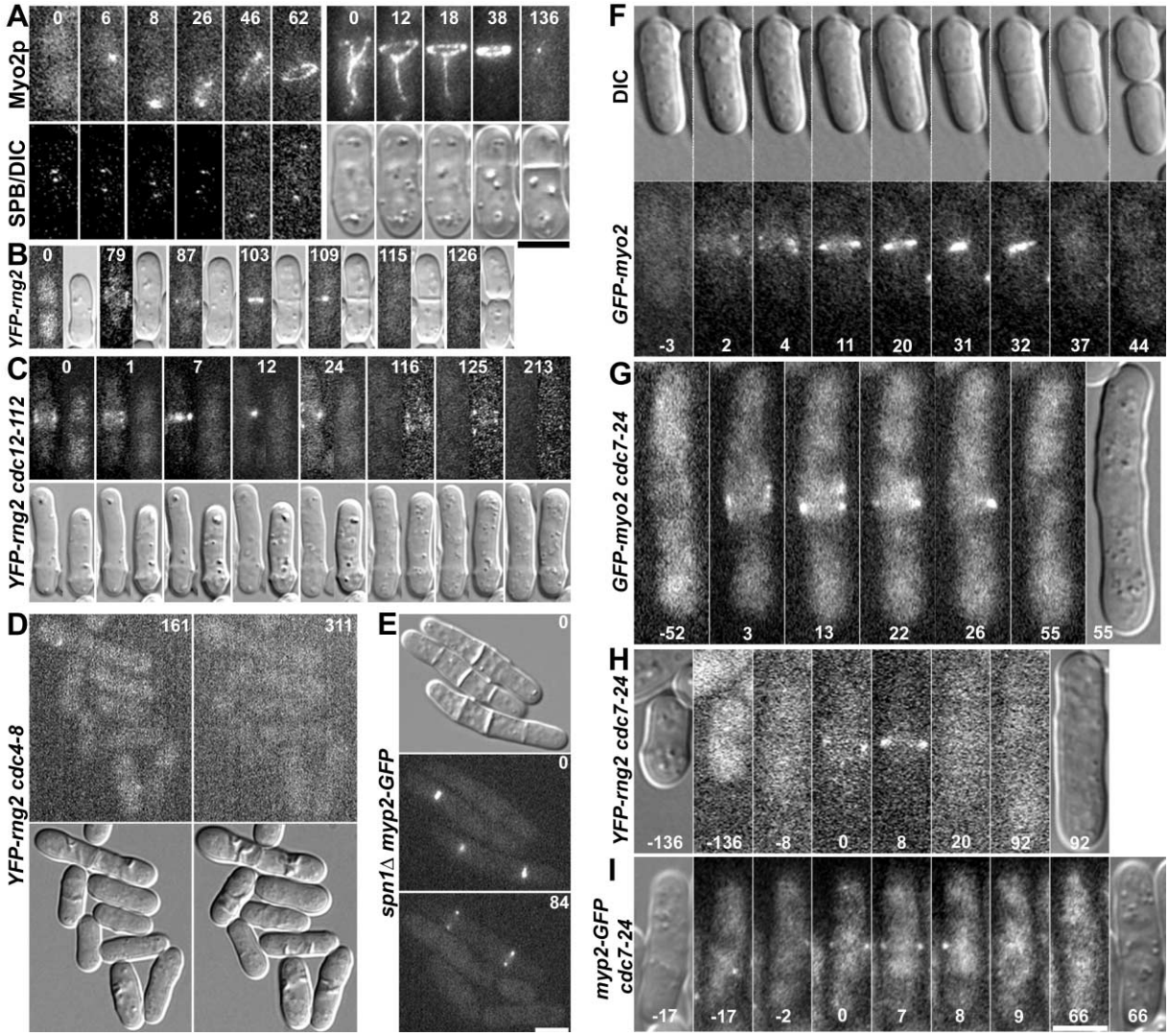


Figure 7. Genetic Dependencies for Localization of Contractile Ring Proteins Observed by Time-Lapse Microscopy

Elapsed times are given in minutes.

(A) Test of dependence of Myo2p localization on Mid1p. Strain *YFP-myo2 sad1-CFP mid1-ΔF* (JW856) with a deletion of anillin *mid1* was grown and observed in EMM2 plus 25% gelatin at 25°C. Left cell: YFP-Myo2p fluorescence micrographs (upper panels) paired with Sad1p-CFP fluorescence. The SPBs separate at time zero. Right cell: YFP-Myo2p fluorescence (upper panels) paired with DIC. The spindle had broken down before the start of the movie at time zero. Eight fluorescence z-sections spaced at 0.7 μm were projected into 2D images using a maximum intensity projection. Two similar series can be viewed in Supplemental Movies 4 and 5.

(B) Control time course of cytokinesis at 36°C in a strain expressing integrated *YFP-rng2* from its native promoter (JW937). Pairs of YFP fluorescence (left) and DIC (right) micrographs. Cells were grown in YE5S liquid medium at 25°C, loaded onto a slide with YE5S plus 2% agar, and sealed. An objective heater warmed the cells from 25°C to 36°C over 20 min beginning at time zero.

(C) Test of dependence of YFP-Rng2p localization on Cdc12p. Strain *YFP-rng2 cdc12-112* (JW954) with a temperature-sensitive mutation in the formin *cdc12* was treated as in (B). Upper: YFP-Rng2p fluorescence; lower: DIC. At time zero (the beginning of the movie), the left cell had a broad band and the right cell had no concentration of YFP-Rng2p.

(D) Test of dependence of YFP-Rng2p localization on Cdc4p. Strain *YFP-rng2 cdc4-8* (JW970-1) with a temperature-sensitive mutation in myosin light chain *cdc4* was grown in liquid EMM2 minimal medium at 25°C, sealed on a slide in EMM2 plus 2% agar, and warmed with an objective heater to 36°C beginning at zero min. The movie began at 160 min. Pairs of YFP fluorescence (upper) and DIC (lower) micrographs. Another 19 cells behaved the same way in a 2 hr movie that started 45 min after the shift to 36°C.

(E) Test of dependence of Myp2p localization on septins. Strain *myp2-GFP spn1Δ* (JW728-1) with a deletion of septin was observed in EMM2 plus 25% gelatin at 25°C. Top: DIC; middle and bottom: Myp2p-GFP fluorescence.

(F–I) Dependence of the localization of type II myosins and IQGAP Rng2p on the SIN pathway. The cells were observed at 36°C in EMM2 plus 2% agar.

(F) Control time course of cytokinesis of a cell expressing GFP-Myo2p (strain JW766) at 36°C. The cell was preincubated on the slide for 2.5 hr at 36°C before the recording. Upper: DIC; lower: fluorescence micrographs.

(G) Test of dependence of GFP-Myo2p localization on SIN. Strain *GFP-myo2 cdc7-24* (JW778) with a temperature-sensitive mutation in the Cdc7p kinase was preincubated on the slide at the restrictive temperature of 36°C for 5 hr to inactivate Cdc7p. Care was taken to maintain the temperature at 36°C before the start of the movie. Zero min is defined as the time of appearance of a broad band of Myo2p. The DIC micrograph was taken at 55 min. The entire series can be viewed in Supplemental Movie 6.

Myp2p does not depend on septins for localizing to the contractile ring. Myp2p localizes normally to the contractile ring in *spn1*$\Delta$ cells (Figure 7E). This deletion prevents all other septins from localizing to the equator and delays separation (J. Pringle, personal communication).

Myo2p localizes to the contractile ring in the absence of SIN pathway activity. The septation initiation network (SIN) consisting of a GTPase and three protein kinases is essential for septation (Guertin et al., 2002; Rajagopalan et al., 2003), but its role in contractile ring assembly is ambiguous. The SIN pathway is not required for anillin Mid1p localization or actin ring formation (Guertin et al., 2002; Rajagopalan et al., 2003; Sohrmann et al., 1996), but one group (Mulvihill et al., 2001) reported that the SIN pathway is required for targeting Myo2p-GFP to the contractile ring. We find that their Myo2p-GFP construct is only partially functional. A new strain with *GFP-myo2* replacing *myo2*$^+$ supports the same time course of mitotic and cytokinetic events at 36°C as untagged wild-type cells (Figure 7F; n = 15 cells). We tested for dependence on the SIN pathway using temperature-sensitive mutation in a SIN pathway kinase, *cdc7-24*. In a *cdc7-24* strain at the restrictive temperature of 36°C, 9 out of 12 cells continue to form broad bands and rings of GFP-Myo2p (Figure 7G; Supplemental Movie 6), but these rings usually collapse into a dot and persist for 38–160 min and no septal material appears at the equator within 3 hr (Figure 7G, DIC). This confirms that the SIN pathway is inactive. Thus, the SIN pathway is required for constriction of the contractile ring and septation but not for localization of Myo2p at the equator.

Rng2p localizes to the contractile ring without the SIN pathway. YFP-Rng2p localized to the division site in three of four *cdc7-24* cells shifted to 36°C for 3 hr (Figure 7H, 0 min, and data not shown). These cells had divided just before the temperature shift. The Rng2p ring stays at the division site for 20 min and then disappears. These cells do not deposit a septum even 1 hr later (Figure 7H).

Localization of Myp2p to the cleavage furrow does not depend on the SIN pathway. Myp2p joined the contractile ring in 9 of 17 asynchronous *cdc7-24* cells over 98 min observations at 36°C, but the cells did not deposit a septum (Figure 7I). These rings collapsed to a dot after 9 min and then disappeared or left the division site 5 min later.

## Discussion

Our analysis of the sequence of events in cytokinesis in fission yeast helps organize information on the process from previous studies. We see that cytokinesis takes place in four precisely timed, sequential stages involving the progressive assembly of more complex structures. All of the events along this time line have the same temperature dependence and high activation energy. The gaps in our knowledge noted in the following summary make the point that understanding the mechanism of cytokinesis will require extensive analysis of molecular interactions as well as continuing work at the cellular level. We focus on 12 contractile ring proteins but recognize that other proteins contribute to cytokinesis including Arp2/3 complex (Arai et al., 1998; Pelham and Chang, 2002), fimbrin Fim1p (Wu et al., 2001), PCH protein Imp2p (Demeter and Sazer, 1998), profilin Cdc3p (Balasubramanian et al., 1994), and Rho GTPases (Arellano et al., 1999).

The first stage sets up a broad equatorial band of proteins that will later form the contractile ring. From midinterphase through the onset of mitosis, the anillin-like protein Mid1p exits progressively from the nucleus and concentrates in the adjacent cortex. Polo kinase Plo1p presumably triggers the release of Mid1p from the nucleus (Bähler et al., 1998a), but neither the release mechanism nor the Mid1p binding site in the cortex are known. At the G2/M transition, this broad band of Mid1p is joined by conventional myosin-II (Myo2p, Cdc4p, and Rlc1p) and IQGAP Rng2p, followed by PCH protein Cdc15p and formin Cdc12p. Equatorial accumulation of these proteins depends on Mid1p but not actin filaments. Direct interactions of these proteins with Mid1p would be the simplest mechanism, but adapters may be involved. The delay between the formation of the broad band of Mid1p and the association of these other proteins (already present in the cytoplasm) shows that an uncharacterized mechanism inhibits these interactions until the G2/M transition. Unmasking or maturation of protein anchoring sites on Mid1p would be a simple mechanism. Assembly reactions downstream of Mid1p can operate in its absence, although imperfectly, forming aberrant, improperly localized contractile rings later than in the presence of Mid1p. Because Myo2p is insoluble at physiological salt concentrations (Bezanilla and Pollard, 2000), the small dots of myosin-II in the broad band may be myosin filaments. IQGAP may be bound to myosin-II, perhaps through Cdc4p (D'souza et al., 2001), because its localization depends on Cdc4p. Nothing is known about molecular anchors for PCH protein (Cdc15p) and formin (Cdc12p) in the broad band.

The brief second stage occurs early in mitosis through anaphase A. Actin filaments (Arai and Mabuchi, 2002) and tropomyosin Cdc8p first join the broad band, and then the band coalesces into a compact ring that includes $\alpha$-actinin Ain1p by a mechanism that depends on actin filaments. Identifying the signal that triggers formin Cdc12p to polymerize actin (Kovar et al., 2003) may reveal how the timing of this stage is controlled. Tropomyosin and $\alpha$-actinin should bind spontaneously to these actin filaments as they polymerize. Interaction of actin filaments with myosin-II is a possible source of force for these movements (Naqvi et al., 1999). Bundling

(H) Test of dependence of YFP-Rng2p localization on SIN. Strain *YFP-rng2 cdc7-24* (JW962-1) was grown at 25°C and warmed to the restrictive temperature of 36°C on the slide at time −180 min. Zero min is defined as the time of appearance of a broad band of Rng2p. DIC micrographs were taken at −136 and 92 min.

(I) Test of dependence of Myp2p-GFP localization on SIN. Strain *myp2-GFP cdc7-24* (JW862-1) was grown at 25°C and warmed to the restrictive temperature of 36°C on the slide for 4 hr prior to observation. Care was taken to maintain the temperature at 36°C before the start of the movie. Zero min is defined as the time of appearance of a ring of Myp2p. DIC micrographs were taken at −17 and 66 min.

of actin filaments by the crosslinking protein α-actinin may also contribute to forming the parallel array of actin filaments in the cleavage furrow (Kanbe et al., 1989). The coalescence of the broad band into the contractile ring resembles the shrinkage of the cortical cytoplasm flanking the equator observed at this time in animal cells (Schroeder, 1972; Rappaport and Rappaport, 1976).

During the prolonged third stage in anaphase B, the compact contractile ring matures by addition of unconventional type II myosin Myp2p and association of septins. Myp2p presumably binds to the actin filaments, but the binding site for septins is not known. A small amount of capping protein Acp2p joins the ring, but most remains in actin patches that cluster near the equator. An unknown mechanism prevents the constriction of the ring during this 25 min interval.

After the mitotic spindle breaks down, the contractile ring constricts and disassembles during the fourth stage. These events depend on the SIN pathway but the connections between the SIN proteins and the contractile ring proteins are not known (Guertin et al., 2002). Proteins dissociate selectively from the ring as it constricts. Actin binding proteins are shed in proportion to the loss of contractile ring volume, while myosin-II becomes more concentrated in the ring during contraction. The mechanisms controlling the dynamics of the various ring proteins have not been studied, although photobleaching experiments have established that the ring proteins turn over rapidly (Pelham and Chang, 2002).

### Comparison with Cytokinesis in Other Organisms

Given that budding and fission yeast diverged from each other only half as long ago (about 400 million years) as fungi diverged from animals, it is remarkable that cytokinesis of fission yeast appears to be more similar to animals than budding yeast. Fungi and animal cells use similar proteins for cytokinesis, but the process appears to be regulated differently in budding yeast from animals and fission yeast. The most obvious difference is that budding yeast specify the division site by the selection of a bud site early in the cell cycle, whereas animals and fission yeast specify a cleavage site midway between the poles of the mitotic spindle with signals emanating from the mitotic apparatus and/or the nucleus (Guertin et al., 2002). Temporally, the only aspect of cytokinesis shared by the two fungi and animal cells is the assembly of a ring of actin filaments around the cleavage site early in mitosis.

Septins take the lead in *S. cerevisiae*, concentrating at the future division site in late G1 phase. Septins are required to recruit the various ring proteins, including the formin Bnr1p in late G1, myosin-II heavy chain Myo1p during G1/S, and PCH protein Hof1p/Cyk2p at G2/M (Bi et al., 1998; Gladfelter et al., 2001; Lippincott and Li, 1998; Vallen et al., 2000). IQGAP Iqg1p/Cyk1p and actin filaments join the ring in anaphase. In contrast, *S. pombe* septins (including Spn1p) appear at the division site late in anaphase B and are not required for localization of any of the 11 contractile ring proteins that we studied for cytokinesis.

The role of myosin-II in budding yeast also differs from fission yeast and animal cells. Myo1p, the only myosin-II in budding yeast, is essential for cytokinesis in some but not all strains (Bi et al., 1998; Lippincott and Li, 1998; Tolliday et al., 2003). Although Myo1p recruits actin and forms a contractile ring (Bi et al., 1998; Lippincott and Li, 1998), the ring lacks conventional myosin-II. Sequence comparisons suggest that Myo1p is an "unconventional" myosin-II related to fission yeast Myp2p (Bezanilla and Pollard, 2000), which is not essential for cytokinesis of fission yeast under most conditions and is not present in animals (Bezanilla et al., 1997). Budding yeast lack conventional myosin-II, which is essential for cytokinesis in fission yeast and animal cells.

Cytokinesis in animal cells and fission yeast appear to have much in common. Less is known in protozoa, but the process seems to be similar. Anillin accumulates in the nucleus during interphase and is the first contractile ring protein known to move to the equator. The timing differs slightly: *S. pombe* anillin moves from the nucleus to the equator starting in G2 and completing in prometaphase, while *Drosophila* anillin does so when the nuclear envelope breaks down in prometaphase (Field and Alberts, 1995). Conventional myosin-II is essential for cytokinesis in fission yeast (Kitayama et al., 1997), animals (Mabuchi and Okuno, 1977), and protozoa (DeLozanne and Spudich, 1987). In fission yeast, animals, and protozoa, conventional myosin-II assembles at the division site before or early in mitosis (Fujiwara and Pollard, 1976) followed shortly by formins (Afshar et al., 2000), α-actinin (Fujiwara et al., 1978), and tropomyosin (Clayton and Johnson, 1998). In many animal cells and protozoa, a cortical meshwork of actin filaments exits prior to assembly of the ring, so the de novo assembly of actin filaments is less conspicuous than in fungi. As in fission yeast, septins join the cleavage furrows of animal cells relatively late in anaphase (Nguyen et al., 2000). In the few cases where it has been measured, the actin component of the ring disassembles (Figure 4C; Schroeder 1972) while the myosin-II becomes concentrated (Figure 4C; Robinson et al., 2002) during constriction of the contractile ring.

Knowledge of the temporal and spatial pathway for assembly and constriction of the contractile ring in fission yeast confronts us with many questions about the process. We hope that answering some of these questions will clarify the mechanisms of cytokinesis in other cell types.

## Experimental Procedures

### Strains, Growth Conditions, and Cellular, Genetic, and Molecular Biology Methods

Supplemental Table S3 lists the *S. pombe* strains used in this study. Standard media and genetic methods are used (http://www.bio.uva.nl/pombe/handbook; Wu et al., 2001). Most genes were tagged with fluorescent fusion proteins at their chromosomal loci by PCR-based gene targeting using *kanMX6* as the selectable marker (Bähler et al., 1998b; Wu et al., 2001). Positives were confirmed by PCR over both junctions and in some cases across the whole integration fragment. With the exception of YFP-Myp2p, YFP-Cdc4p, Cdc15p-GFP, and Cdc15p-YFP, all of the tagged proteins presented in this paper were functional by several criteria: colony growth, generation time, and morphology at different temperatures; crosses with mutations known to give synthetic phenotypes; and growth under stressful conditions known to elicit a phenotype from a mutation in the gene. GFP tagging compromised the function of some proteins of interest: either end of profilin (Cdc3p) and actin Act1p; chromosomal COOH-terminal tagged myosin II *myo2*, IQGAP *rng2*, and tropomyosin *cdc8*; and chromosomal $NH_2$-terminal tagged *cdc8*, so these

constructs could not be included in this study. See Supplemental Data at http://www.developmentalcell.com/cgi/content/full/5/5/723/DC1 for full documentation.

To determine the effects of actin depolymerization on protein localization, cells were grown to 2–5 $\times$ $10^6$ cells/ml. Lat-A (Molecular Probes) was added from a 20 mM stock solution in DMSO to a final concentration of 100 $\mu$M (0.5% DMSO). Control cultures were treated with 0.5% DMSO.

### Microscopy and Data Analysis

Cells were observed by fluorescence and differential-interference-contrast (DIC) microscopy using an Olympus IX-71 inverted microscope equipped with a 60$\times$ 1.4 NA Plan-apo objective, appropriate filter sets (DIC, CFP, FITC, and YFP), and a Hamamatsu Orca-ER cooled CCD camera (Bridgewater, NJ) for all experiments except Figure 3, which used an Ultraview spinning disk confocal microscope (Perkin Elmer Life Sciences). Details are described in Supplemental Data.

### Acknowledgments

This work was supported by National Institutes of Health grant GM-26231 to T.D.P., a Career Award at the Scientific Interface from the Burroughs Wellcome Fund to J.R.K., and an NIH NRSA fellowship to D.R.K. We thank Matthew Lord for *rlc1* strains; Chris Beltzner and Chloé Diamond for help with making integration plasmids; Chloé Diamond for making some strains; Volodia Sirotkin for help with making actin plasmids; Zina Gorelik for technical assistance; and members of our lab for helpful discussions. We are grateful to Fred Chang for pFA6a-YFP-kanMX6, pFA6a-CFP-kanMX6, pUR19-41nmt1-cdc12-CFP, and pREP3X-CFP-tubulin plasmids; Mohan Balasubramanian for pREP42-GFP-cdc8 plasmid; and John Pringle for septin strains and helpful comments on the manuscript.

Received: August 21, 2003
Revised: September 30, 2003
Accepted: October 2, 2003
Published: November 3, 2003

### References

Afshar, K., Stuart, B., and Wasserman, S.A. (2000). Functional analysis of the *Drosophila* diaphanous FH protein in early embryonic development. Development *127*, 1887–1897.

Arai, R., and Mabuchi, I. (2002). F-actin ring formation and the role of F-actin cables in the fission yeast *Schizosaccharomyces pombe*. J. Cell Sci. *115*, 887–898.

Arai, R., Nakano, K., and Mabuchi, I. (1998). Subcellular localization and possible function of actin, tropomyosin and actin-related protein 3 (Arp3) in the fission yeast *Schizosaccharomyces pombe*. Eur. J. Cell Biol. *76*, 288–295.

Arellano, M., Coll, P.M., and Perez, P. (1999). RHO GTPases in the control of cell morphology, cell polarity, and actin localization in fission yeast. Microsc. Res. Tech. *47*, 51–60.

Ayscough, K.R., Stryker, J., Pokala, N., Sanders, M., Crews, P., and Drubin, D.G. (1997). High rates of actin filament turnover in budding yeast and roles for actin in establishment and maintenance of cell polarity revealed using the actin inhibitor latrunculin-A. J. Cell Biol. *137*, 399–416.

Bähler, J., and Pringle, J.R. (1998). Pom1p, a fission yeast protein kinase that provides positional information for both polarized growth and cytokinesis. Genes Dev. *12*, 1356–1370.

Bähler, J., Steever, A.B., Wheatley, S., Wang, Y., Pringle, J.R., Gould, K.L., and McCollum, D. (1998a). Role of polo kinase and Mid1p in determining the site of cell division in fission yeast. J. Cell Biol. *143*, 1603–1616.

Bähler, J., Wu, J.-Q., Longtine, M.S., Shah, N.G., McKenzie, A., III, Steever, A.B., Wach, A., Philippsen, P., and Pringle, J.R. (1998b). Heterologous modules for efficient and versatile PCR-based gene targeting in *Schizosaccharomyces pombe*. Yeast *14*, 943–951.

Balasubramanian, M.K., Helfman, D.M., and Hemmingsen, S.M. (1992). A new tropomyosin essential for cytokinesis in the fission yeast *S. pombe*. Nature *360*, 84–87.

Balasubramanian, M.K., Hirani, B.R., Burke, J.D., and Gould, K.L. (1994). The *Schizosaccharomyces pombe cdc3*$^+$ gene encodes a profilin essential for cytokinesis. J. Cell Biol. *125*, 1289–1301.

Bezanilla, M., and Pollard, T.D. (2000). Myosin-II tails confer unique functions in *Schizosaccharomyces pombe*: characterization of a novel myosin-II tail. Mol. Biol. Cell *11*, 79–91.

Bezanilla, M., Forsburg, S.L., and Pollard, T.D. (1997). Identification of a second myosin-II in *Schizosaccharomyces pombe*: Myp2p is conditionally required for cytokinesis. Mol. Biol. Cell *8*, 2693–2705.

Bezanilla, M., Wilson, J.M., and Pollard, T.D. (2000). Fission yeast myosin-II isoforms assemble into contractile rings at distinct times during mitosis. Curr. Biol. *10*, 397–400.

Bi, E., Maddox, P., Lew, D.J., Salmon, E.D., McMillan, J.N., Yeh, E., and Pringle, J.R. (1998). Involvement of an actomyosin contractile ring in *Saccharomyces cerevisiae* cytokinesis. J. Cell Biol. *142*, 1301–1312.

Carnahan, R.H., and Gould, K.L. (2003). The PCH family protein, Cdc15p, recruits two F-actin nucleation pathways to coordinate cytokinetic actin ring formation in *Schizosaccharomyces pombe*. J. Cell Biol. *162*, 851–862.

Chang, F., Wollard, A., and Nurse, P. (1996). Isolation and characterization of fission yeast mutants defective in the assembly and placement of the contractile actin ring. J. Cell Sci. *109*, 131–142.

Chang, F., Drubin, D., and Nurse, P. (1997). cdc12p, a protein required for cytokinesis in fission yeast, is a component of the cell division ring and interacts with profilin. J. Cell Biol. *137*, 169–182.

Clayton, L., and Johnson, M.H. (1998). Tropomyosin in preimplantation mouse development: identification, expression, and organization during cell division and polarization. Exp. Cell Res. *238*, 450–464.

DeLozanne, A., and Spudich, J.A. (1987). Disruption of the *Dictyostelium* myosin heavy chain gene by homologous recombination. Science *236*, 1086–1091.

Demeter, J., and Sazer, S. (1998). imp2, a new component of the actin ring in the fission yeast *Schizosaccharomyces pombe*. J. Cell Biol. *143*, 415–427.

Ding, R., West, R.R., Morphew, D.M., Oakley, B.R., and McIntosh, J.R. (1997). The spindle pole body of *Schizosaccharomyces pombe* enters and leaves the nuclear envelope as the cell cycle proceeds. Mol. Biol. Cell *8*, 1461–1479.

D'souza, V.M., Naqvi, N.I., Wang, H., and Balasubramanian, M.K. (2001). Interactions of Cdc4p, a myosin light chain, with IQ-domain containing proteins in *Schizosaccharomyces pombe*. Cell Struct. Funct. *26*, 555–565.

Eng, K., Naqvi, N.I., Wong, K.C., and Balasubramanian, M.K. (1998). Rng2p, a protein required for cytokinesis in fission yeast, is a component of the actomyosin ring and the spindle pole body. Curr. Biol. *8*, 611–621.

Fankhauser, C., Reymond, A., Cerutti, L., Utzig, S., Hofmann, K., and Simanis, V. (1995). The *S. pombe cdc15* gene is a key element in the reorganization of F-actin at mitosis. Cell *82*, 435–444.

Feierbach, B., and Chang, F. (2001). Cytokinesis and the contractile ring in fission yeast. Curr. Opin. Microbiol. *4*, 713–719.

Field, C.M., and Alberts, B.M. (1995). Anillin, a contractile ring protein that cycles from the nucleus to the cell cortex. J. Cell Biol. *131*, 165–178.

Fujiwara, K., and Pollard, T.D. (1976). Fluorescent antibody localization of myosin in the cytoplasm, cleavage furrow, and mitotic spindle of human cells. J. Cell Biol. *71*, 848–875.

Fujiwara, K., Porter, M.E., and Pollard, T.D. (1978). $\alpha$-actinin localization in the cleavage furrow during cytokinesis. J. Cell Biol. *79*, 268–275.

Gladfelter, A.S., Pringle, J.R., and Lew, D.J. (2001). The septin cortex at the yeast mother-bud neck. Curr. Opin. Microbiol. *4*, 681–689.

Glynn, J.M., Lustig, R.J., Berlin, A., and Chang, F. (2001). Role of bud6p and tea1p in the interaction between actin and microtubules for the establishment of cell polarity in fission yeast. Curr. Biol. *11*, 836–845.

Guertin, D.A., Trautmann, S., and McCollum, D. (2002). Cytokinesis in eukaryotes. Microbiol. Mol. Biol. Rev. *66*, 155–178.

Kanbe, T., Kobayashi, I., and Tanaka, K. (1989). Dynamics of cytoplasmic organelles in the cell cycle of the fission yeast *Schizosaccharomyces pombe*: three-dimensional reconstruction from serial sections. J. Cell Sci. *94*, 647–656.

Kitayama, C., Sugimoto, A., and Yamamoto, M. (1997). Type II myosin heavy chain encoded by the *myo2* gene composes the contractile ring during cytokinesis in *Schizosaccharomyces pombe*. J. Cell Biol. *137*, 1309–1319.

Kovar, D.R., Kuhn, J.R., Tichy, A.L., and Pollard, T.D. (2003). The fission yeast cytokinesis formin Cdc12p is a barbed end actin filament capping protein gated by profilin. J. Cell Biol. *161*, 875–887.

Le Goff, X., Utzig, S., and Simanis, V. (1999). Controlling septation in fission yeast: finding the middle, and timing it right. Curr. Genet. *35*, 571–584.

Lippincott, J., and Li, R. (1998). Sequential assembly of myosin II, an IQGAP-like protein, and filamentous actin to a ring structure involved in budding yeast cytokinesis. J. Cell Biol. *140*, 355–366.

Mabuchi, I., and Okuno, M. (1977). The effect of myosin antibody on the division of starfish blastomeres. J. Cell Biol. *74*, 251–263.

Mallavarapu, A., Sawin, K., and Mitchison, T. (1999). A switch in microtubule dynamics at the onset of anaphase B in the mitotic spindle of *Schizosaccharomyces pombe*. Curr. Biol. *9*, 1423–1426.

Marks, J., and Hyams, J.S. (1985). Localization of F-actin through the cell division cycle of *Schizosaccharomyces pombe*. Eur. J. Cell Biol. *39*, 27–32.

Motegi, F., Nakano, K., and Mabuchi, I. (2000). Molecular mechanism of myosin-II assembly at the division site in *Schizosaccharomyces pombe*. J. Cell Sci. *113*, 1813–1825.

Mulvihill, D.P., Barretto, C., and Hyams, J.S. (2001). Localization of fission yeast type II myosin, Myo2, to the cytokinetic actin ring is regulated by phosphorylation of a C-terminal coiled-coil domain and requires a functional septation initiation network. Mol. Biol. Cell *12*, 4044–4053.

Nabeshima, K., Nakagawa, T., Straight, A.F., Murray, A., Chikashige, Y., Yamashita, Y.M., Hiraoka, Y., and Yanagida, M. (1998). Dynamics of centromeres during metaphase-anaphase transition in fission yeast: Dis1 is implicated in force balance in metaphase bipolar spindle. Mol. Biol. Cell *9*, 3211–3225.

Naqvi, N.I., Eng, K., Gould, K.L., and Balasubramanian, M.K. (1999). Evidence for F-actin-dependent and -independent mechanisms involved in assembly and stability of the medial actomyosin ring in fission yeast. EMBO J. *18*, 854–862.

Nguyen, T.Q., Sawa, H., Okano, H., and White, J.G. (2000). The *C. elegans* septin genes, *unc-59* and *unc-61*, are required for normal postembryonic cytokineses and morphogenesis but have no essential function in embryogenesis. J. Cell Sci. *113*, 3825–3837.

Nurse, P., Thuriaux, P., and Nasmyth, K. (1976). Genetic control of the cell division cycle in the fission yeast *Schizosaccharomyces pombe*. Mol. Gen. Genet. *146*, 167–178.

Ohkura, H., Hagan, I.M., and Glover, D.M. (1995). The conserved *Schizosaccharomyces pombe* kinase plo1, required to form a bipolar spindle, the actin ring, and septum, can drive septum formation in G1 and G2 cells. Genes Dev. *9*, 1059–1073.

Paoletti, A., and Chang, F. (2000). Analysis of mid1p, a protein required for placement of the cell division site, reveals a link between the nucleus and the cell surface in fission yeast. Mol. Biol. Cell *11*, 2757–2773.

Pelham, R.J., and Chang, F. (2002). Actin dynamics in the contractile ring during cytokinesis in fission yeast. Nature *419*, 82–86.

Rajagopalan, S., Wachtler, V., and Balasubramanian, M. (2003). Cytokinesis in fission yeast: a story of rings, rafts and walls. Trends Genet. *19*, 403–408.

Rappaport, R., and Rappaport, B.N. (1976). Prefurrow behavior of the equatorial surface in *Arbacia lixula* eggs. Dev. Growth Differ. *18*, 189–193.

Robinson, D.N., Cavet, G., Warrick, H.M., and Spudich, J.A. (2002). Quantitation of the distribution and flux of myosin-II during cytokinesis. BMC Cell Biol. *3*, 4.

Schroeder, T.E. (1972). The contractile ring. II. Determining its brief existence, volumetric changes, and vital role in cleaving *Arbacia* eggs. J. Cell Biol. *53*, 419–434.

Sohrmann, M., Fankhauser, C., Brodbeck, C., and Simanis, V. (1996). The *dmf1/mid1* gene is essential for correct positioning of the division septum in fission yeast. Genes Dev. *10*, 2707–2719.

Tolliday, N., Pitcher, M., and Li, R. (2003). Direct evidence for a critical role of myosin II in budding yeast cytokinesis and the evolvability of new cytokinetic mechanisms in the absence of myosin II. Mol. Biol. Cell *14*, 798–809.

Vallen, E.A., Caviston, J., and Bi, E. (2000). Roles of Hof1p, Bni1p, Bnr1p, and Myo1p in cytokinesis in *Saccharomyces cerevisiae*. Mol. Biol. Cell *11*, 593–611.

Wong, K.C.Y., Naqvi, N.I., Lino, Y., Yamamoto, M., and Balasubramanian, M.K. (2000). Fission yeast Rng3p: an UCS-domain protein that mediates myosin II assembly during cytokinesis. J. Cell Sci. *113*, 2421–2432.

Wu, J.-Q., Bähler, J., and Pringle, J.R. (2001). Roles of a fimbrin and an $\alpha$-actinin-like protein in fission yeast cell polarization and cytokinesis. Mol. Biol. Cell *12*, 1061–1077.